Proceedings of the 4th International Conference on Signal Processing and Machine Learning
DOI: 10.54254/2755-2721/49/20241550

Research on space power supply utilizing series-parallel techniques

Wu Haonan

School of Electric Power, South China University of Technology, Guangzhou, China

202030233148@mail.scut.edu.cn

Abstract. In the realm of space exploration, maintaining a stable and reliable power supply is crucial for the sustained and uninterrupted operation of artificial satellites. However, the unpredictable and often harsh space environment necessitates a redundant design for space power supplies to enhance overall reliability. In light of this, this paper introduces a full-bridge converter employing a series-parallel topology, which augments input voltage redundancy through a combination of serial and parallel connections. Furthermore, a dual-loop Proportional-Integral (PI) control feedback system has been devised, along with a comprehensive analysis of system stability to ensure the optimal performance of both output voltage and current. To validate the efficacy of the series-parallel topology and the feedback system, a complete circuit is constructed, and extensive simulations are carried out under diverse conditions.

Keywords: space power supply, full-bridge converter, series-parallel topology, dual-loop feedback

1. Introduction

Space power supply, as the primary source of electrical energy for artificial satellites in space, is integral to ensuring their sustained and stable operation. Instabilities in space power supplies can significantly disrupt the normal functioning of satellite components. Therefore, research on space power supply systems is imperative. Currently, solar panels are the most commonly used system [1]. These panels harness solar energy and convert it into unstable electrical energy, which is subsequently transformed into a stable output electrical energy through a DC-DC converter.

In the realm of space power supply systems, there is a growing demand for high voltage and high power converters [2]. The primary high-power converters include full-bridge converters, Weinberg converters, and super boost converters. However, Weinberg converter may exhibit voltage oscillations, resulting in significant switching losses. The super boost converter system's topology is nonlinear, with a second-order transfer function [3]. Considering the relatively high stability of the full-bridge converter in space environments and its ability to achieve high voltage and high power output objectives [4], this paper selects the full-bridge converter as the primary topology to encompass the functionalities of the mentioned converters. Given the discontinuous and unstable nature of solar panel output voltage, the control circuit design of this converter typically incorporates a negative feedback regulation system to stabilize the output voltage [5].

In the unpredictable space environment, critical component failures may occur within the space power supply system. Consequently, research on space power supply systems with redundant designs

DOI: 10.54254/2755-2721/49/20241550

and robust anti-interference capabilities is of paramount significance [6]. This paper introduces a series-parallel full-bridge converter topology where two sets of solar panels are connected in parallel at the input, operating independently, and then connected in series at the output to increase the available voltage and power output. This configuration ensures that in the uncertain space environment, if one solar panel experiences insufficient or no output, the other independent solar panel remains unaffected and can continue to provide sufficient voltage.

In summary, this paper presents a series-parallel full-bridge converter with a negative feedback regulation circuit and validates its operational performance and stability. It offers theoretical support for related research and design endeavors.

2. Analyse of Series-Parallel Full-Bridge Converter

2.1. Introduction to the Series-Parallel Topology

The principal circuit diagram of the series-parallel full-bridge converter is illustrated in Figure 1. On the left-hand side, two identical full-bridge input sections are employed, with two solar panels serving as the input voltage sources.

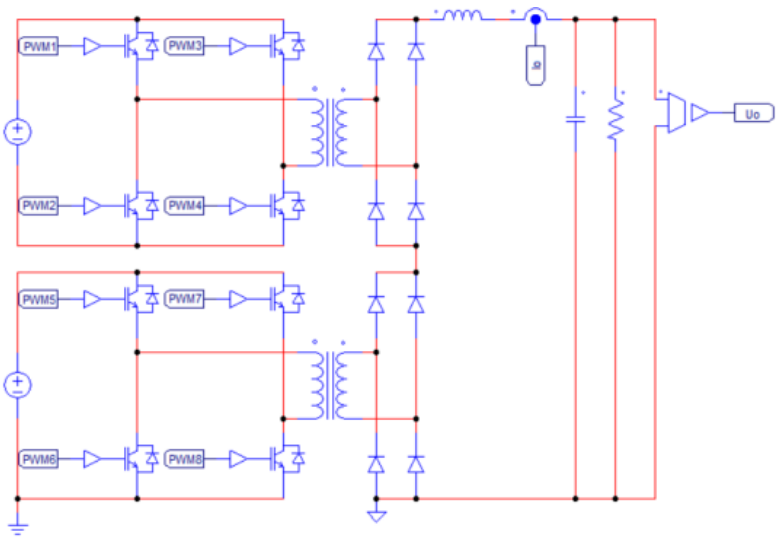

Figure 1. Structure diagram of series-parallel topology

The design of the input in parallel and output in series topology effectively guarantees the output voltage level while enhancing the overall power output. Simultaneously, the redundant parallel input design bolsters the converter's reliability. Under the control of the negative feedback system, if one solar panel's output proves insufficient, the other solar panel's normal operation can still guarantee an adequate voltage level for the load.

2.2. Principle Analysis and Parameter Design

In the complementary turn-on mode with two groups of 8 IGBTs, this converter effectively transforms unstable DC voltage from the solar panel into a stable DC voltage at the load. The circuit's conduction status is depicted in the red circuit in Figure 2.

DOI: 10.54254/2755-2721/49/20241550

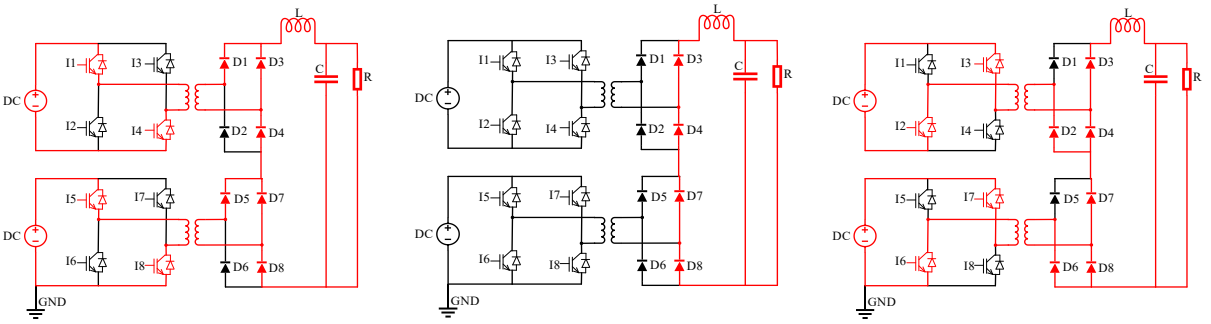

(a) The first stage (b) The second and the forth stage (c) The third stage

Figure 2. Conduction condition in all stages

The objective of the converter in this study is to convert the unstable DC voltage from the solar panels, which ranges from 170V to 250V, into a stable DC voltage of 350V. Consequently, the subsequent parameter design is based on this established objective for calculation and selection.

2.2.1. Transformer

Given the need for both independent solar panel inputs to approach the output voltage target value after boosting, the turns ratio k is determined by Equation (1).

$$k = \frac{U_o}{U_{i\min}} \tag{1}$$

Here, when the input voltage is at its minimum of 170V, the transformer's turns ratio can still achieve a sufficient output voltage level close to 350V. Therefore, a turns ratio of $k=2$ is selected.

2.2.2. Load Resistance

To meet the output voltage and power requirements, a resistance value of $R=12\Omega$ is chosen.

2.2.3. Continuous Current Inductance

To ensure continuous current flow under all circumstances, the required inductance value is calculated at the maximum input voltage [7]. The ripple amount of the inductance current is assumed to be 10% of the output current, and since the rated output voltage and output power are determined, the output current is set to be around 30A. U_{Lmax} represents the maximum voltage across the inductance, and U_{2max} represents the maximum voltage at the secondary side of the circuit. f represents the IGBT switch frequency, set at 10kHz. U_o represents the rated output voltage, set at 350V. The size of the output continuous current inductance L is determined by Equation (2).

$$L = \frac{U_{L\max}}{\Delta I_L} D_{on} T = \frac{U_{2\max} - U_o}{10\% I_o} \frac{U_o}{f U_{2\max}} \tag{2}$$

Here, the value of L is calculated to be 7.58mH. With a margin in mind, $L=10mH$ is selected for this paper.

2.2.4. Load Capacitance

Given that the ripple frequency f_c of the output capacitance voltage is twice the switching frequency and that the ripple ratio of the output voltage for the full-bridge converter is generally 0.05%, the load capacitance size is determined by Equation (3) [8].

$$C = \frac{\Delta I_o}{8 f_c \Delta U_o} \tag{3}$$

DOI: 10.54254/2755-2721/49/20241550

The calculated value is *C=107.14uF*, but for added margin, this paper opts for *C=120uF*.

2.3. Closed-Loop Control System and Its Stability Analysis

As illustrated in Figure 3, the feedback control circuit of the converter is utilized, employing a dual-loop PI controller for regulation.

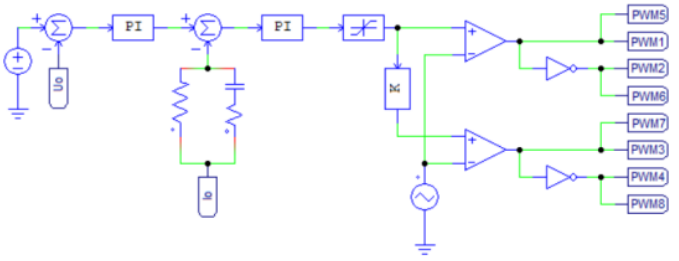

Figure 3. Circuit diagram of dual-loop PI control system

The outer loop control focuses on regulating the output voltage of the load. Serving as the primary feedback control loop, it stabilizes the output voltage even in the presence of fluctuations in the converter's input. The inner loop control pertains to the regulation of inductance current at the converter's output. This inner loop effectively maintains the magnitude of the inductance current.

The system structure diagram of the converter under dual-loop negative feedback control is presented in Figure 4.

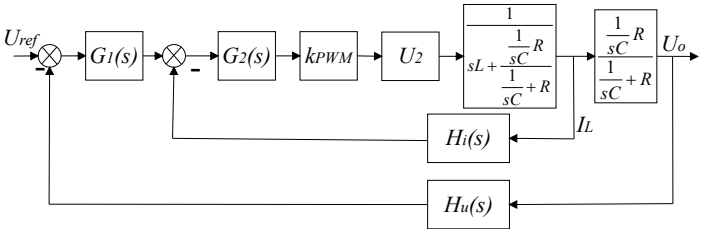

Figure 4. System structure diagram

The current inner loop encompasses the PI controller $G_2(s)$, PWM control coefficient k_{PWM}, transformer secondary voltage U_2, output terminal of the *RLC* series-parallel structure, and current feedback loop. The transfer function of the PI controller is articulated in Equation (4).

$$G_2(s) = \frac{k_2(1+T_2 s)}{T_2 s} \tag{4}$$

The specific parameter values are k2 = 0.1 and T2 = 0.002.

The PWM control coefficient is defined as the ratio of the circuit's output voltage to the voltage output of the current PI controller. During the simulation, the voltage output of the current PI controller is measured to be Upi = 0.35V at steady state. Consequently, the value of kPWM is calculated to be 1000. Since the secondary voltage of the transformer fluctuates with changes in input voltage, we take the average value of the transformer's secondary voltage, and U2 is computed to be 840V.

The current loop feedback coefficient Hi(s) is set at 0.005. Consequently, with all parameters available, we can determine the open-loop transfer function, as demonstrated in Equation (5).

$$G_i(s) = G_2(s) k_{PWM} U_2 \frac{1}{sL + \dfrac{\dfrac{1}{sC} R}{\dfrac{1}{sC} + R}} H_i(s) \tag{5}$$

DOI: 10.54254/2755-2721/49/20241550

The voltage outer loop involves a PI controller $G_1(s)$, a simplified current inner loop system, an RC load, and a voltage feedback loop. The transfer function of the voltage outer loop PI controller is detailed in Equation (6).

$$G_1(s) = \frac{k_1(1+T_1 s)}{T_1 s} \tag{6}$$

The specific parameter values are: k1=0.007 and T1=0.009.

The voltage feedback coefficient Hu(s) is set at 1. This permits the derivation of the open-loop transfer function of the voltage outer loop, articulated in Equation (7).

$$G_u(s) = G_1(s)\frac{\frac{1}{sC}R}{\frac{1}{sC}+R}\Phi_i(s)H_u(s) \tag{7}$$

Reference [9] suggests using Bode plots to evaluate the system stability of a DC-DC converter. Consequently, Bode plots of the open-loop transfer functions are generated in MATLAB, as exhibited in Figure 5.

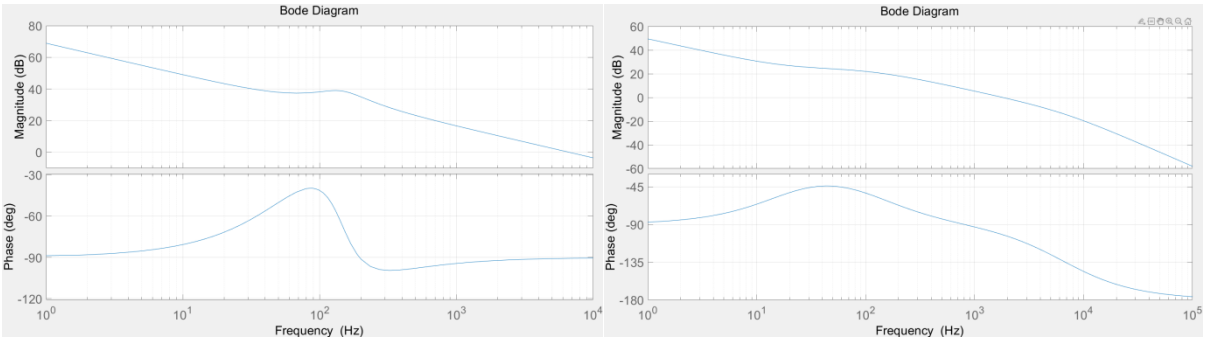

(a) Current loop (b) Voltage loop

Figure 5. Bode plots of the open-loop transfer functions

In combination with the obtained Bode plot and the system stability analysis methods presented in reference [10], in the current loop, it is evident that at the cutoff frequency, the phase margin reaches 90°, and the Bode plot curve indicates a favorable gain margin. Similar to the current loop analysis, it can be observed from the curve trend that the voltage loop boasts a favorable phase margin of 90° and a gain margin of approximately 60dB.

In conclusion, the analysis affirms that the open-loop characteristics of the designed dual-loop feedback system adhere to the fundamental requirements for system stability.

3. Simulation process and result verification

3.1. Simulation Condition Setting

Given the high-frequency characteristics of power electronic devices, such as IGBT, which typically operate at frequencies ranging from a few kilohertz to several tens of kilohertz [11], this article will utilize a 10kHz unipolar isosceles triangular waveform with an amplitude of 1V and a duty cycle of 0.5 as the carrier signal for the PWM signal generation circuit in this topology.

3.2. Simulation Results

In this study, the circuit is constructed in the PSIM simulation software. The circuit's reliability is assessed by monitoring the output voltage, output current, and output current ripple under different input conditions. The design objectives for this topology involve delivering a stable output voltage of 350V

DOI: 10.54254/2755-2721/49/20241550

while the input voltage from the two solar panel arrays varies between 170V and 250V. To swiftly verify the circuit's reliability under these conditions, three different input scenarios of the two solar panel arrays are simulated: 170V with 170V, 170V with 250V, and 250V with 250V.

3.2.1. Result Analysis of Output Voltage

The output voltage results under these three conditions are presented in Figure 6.

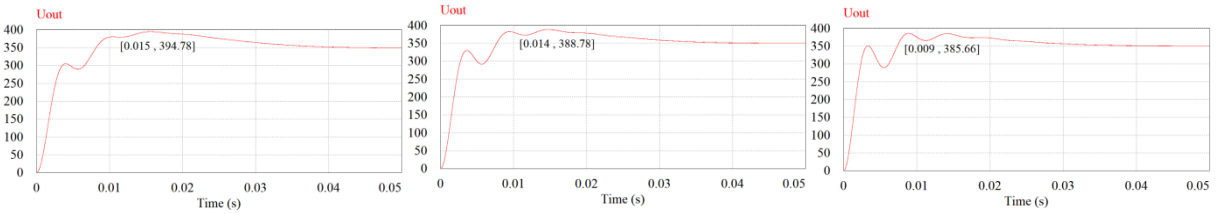

(a) 170V with 170V (b) 170V with 250V (c) 250V with 250V

Figure 6. Waveform diagrams of output voltage in different input scenarios

Using PSIM's measurement function, the maximum value of the output voltage within the feedback response time is determined for the three cases. The calculated overshoots are 12.79%, 11.08%, and 10.19%, respectively. In alignment with the description of the PI control system in reference [12], these overshoot values meet the basic requirements. Additionally, the result graph shows that the time for the output voltage to reach and stabilize at the target value typically falls between 0.04s and 0.05s. This indicates that the PI feedback control system exhibits strong dynamic response capabilities.

3.2.2. Result Analysis of Output Current

This simulation assesses the inductance current at the output as the output current and measures its magnitude and ripple size to verify the reliability of the current control loop. The waveform of the output current for the three cases is displayed in Figure 7.

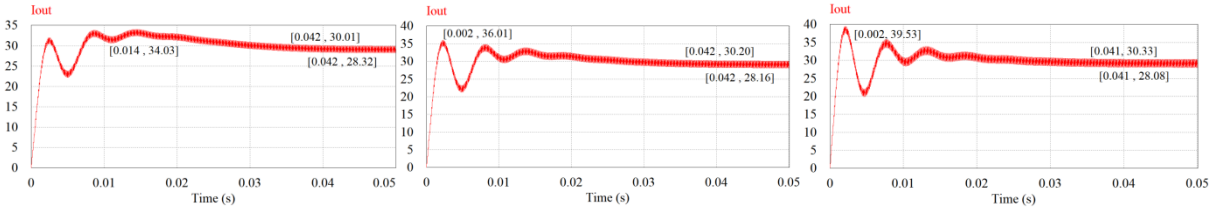

(a) 170V with 170V (b) 170V with 250V (c) 250V with 250V

Figure 7. Waveform diagrams of output current in different input scenarios

By analyzing the measured data, the overshoot and ripple magnitude of the output current can be calculated, and the measured values are shown in Figure 7. After analyzing the data, the calculated overshoots are 16.7%, 22.19%, and 35.26%, respectively. And the calculated ripple coefficients of the output current are 5.8%, 6.9%, and 7.7%, respectively. The ripple coefficient of the output current meets the requirements, and the maximum overshoot of the output current is 35%, which essentially aligns with the requirements.

4. Conclusion

This paper has successfully designed a series-parallel full-bridge converter, established the primary topology and feedback loop, and confirmed the system's stability and the functionality of its core circuit elements.

By employing theoretical calculations and simulation debugging, while adhering to predefined target values for input voltage, output voltage, and output current, the parameters for the series-parallel full-bridge converter with a dual-loop feedback control system have been meticulously derived. Additionally,

DOI: 10.54254/2755-2721/49/20241550

the main topology circuit has been constructed, and the operating principles of this topology have been comprehensively analyzed.

A systematic stability analysis has been conducted, incorporating the open-loop transfer function. This analysis involved the generation of Bode plots, calculation of gain and phase margins, and ultimately, the validation of the stability of the dual-loop current-voltage system.

A series of simulations were executed under three distinct input scenarios. The results encompass measurements of overshoot, steady-state values, and ripple magnitudes of both the output voltage and output current within the topology circuit. These comprehensive assessments serve to confirm the operational efficacy of the core topology circuit and its integrated feedback control system.

References

[1] L.Wang, D.L.Zhang, Senior Member, IEEE, J.P.Duan, J.N.Li, "Design and Research of High Voltage Power Conversion System for Space Solar Power Station", 2018 IEEE International Power Electronics and Application Conference and Exposition, Nov.2018

[2] B.M.Novac, I.R.Smith, P.Senior, M.Parker, G.Louverdis, "High voltage pulsed-power sources for high-energy experimentation", 2010 IEEE International Power Modulator and High Voltage Conference, May.2010

[3] H.Li, S.L.Wu, Y.Jiang, B.Tu, J.J.Ma, W.B.Hu, "Research on Battery Discharge Regulator Based on Weinberg Topology", 2020 IEEE 9th Joint International Information Technology and Artificial Intelligence Conference, Dec.2020

[4] W.J.Zhao, C.A.Wan, Y.F.Gao, "Space High Voltage Power Module Design", 2020 2nd International Conference on Smart Power & Internet Energy Systems, Sep.2020

[5] Md Rasel Mahmud, Hemanshu Pota, "Robust Feedback Linearizing Controller Design for DC Microgrid Connected DC-DC Converter", 2021 IEEE Texas Power and Energy Conference, Feb.2021

[6] Y.Q.Zhang, Z.X.Xu, L.Y.Yan, "Design of redundancy and voltage regulation for the space power system based on DSP", Electronic Measurement Technology, vol.9, No.38, Sep.2015(In Chinese)

[7] Snehal Chothe, Rajaram. T. Ugale, Ameya Gambhir, "Design and modeling of Phase Shifted Full Bridge DC-DC Converter with ZVS", 2021 National Power Electronics Conference, Dec.2021

[8] D.Song, R.P.Ji, "Study of DC-DC Converter for Space Power System" Journal Of Electrical Engineering ,vol.12, No.6,Jun.2017(In Chinese)

[9] Daniel M. Barrera Leguizamón, Robert Urbina, Carlos Páez, Arturo Fajardo, Gabriel Perilla, "On the Bode Diagram Plot of Switched Converters Using MATLAB Simulink - a Tutorial Approach" 2023 IEEE 14th Latin America Symposium on Circuits and Systems, Feb.2023

[10] C.H.Guan, W.J.Li, X.Y.Zhang, Y.Lv, W.W.Yu, "Stability Analysis of Bidirectional DC-DC Converter for Energy Storage", 2019 IEEE 2nd International Conference on Power and Energy Applications , Apr.2019

[11] Shimada.T, Taniguchi.K, "IGBT/MOSFET hybrid bridge with phase shift and frequency modulation control for a bi-directional series resonant converter", 2017 19th European Conference on Power Electronics and Applications, Sep.2017

[12] Elanur Ekici, Tahsin Koroglu, Doğan Çelik, "An Isolated High-Power Bidirectional Five-Level NPC Dual Active Bridge DC-DC Converter with Anti-Windup PI Controller for Electric Vehicle-to-Home Application" 2023 15th International Conference on Electronics, Computers and Artificial Intelligence, Jun.2023